Christian Hirt

# Prediction of vertical deflections from high-degree spherical harmonic synthesis and residual terrain model data

**Abstract** This study demonstrates that in mountainous areas the use of residual terrain model (RTM) data significantly improves the accuracy of vertical deflections obtained from high-degree spherical harmonic synthesis. The new Earth gravitational model EGM2008 is used to compute vertical deflections up to a spherical harmonic degree of 2160. RTM data can be constructed as difference between high-resolution SRTM (Shuttle Radar Topography Mission) elevation data and the terrain model DTM2006.0 (a spherical harmonic terrain model that complements EGM2008) providing the long-wavelength reference surface. Because these RTM elevations imply most of

C. Hirt

Western Australian Centre for Geodesy & The Institute for Geoscience Research

Curtin University of Technology

GPO Box U 1987

Perth, WA 6845, Australia

E-mail: Chris.Hirt@web.de

E-mail: c.hirt@curtin.edu.au

the gravity field signal beyond spherical harmonic degree of 2160, they can be used to augment EGM2008 vertical deflection predictions in the very high spherical harmonic degrees.

In two mountainous test areas - the German and the Swiss Alps - the combined use of EGM2008 and RTM data was successfully tested at 223 stations with high-precision astrogeodetic vertical deflections from recent zenith camera observations (accuracy of about 0.1 arc seconds) available. The comparison of EGM2008 vertical deflections with the ground-truth astrogeodetic observations shows RMS values (from differences) of 3.5 arc seconds for $\xi$ and 3.2 arc seconds for $\eta$, respectively. Using a combination of EGM2008 and RTM data for the prediction of vertical deflections considerably reduces the RMS values to the level of 0.8 arc seconds for both vertical deflection components, which is a significant improvement of about 75 percent. Density anomalies of the real topography with respect to the residual model topography are one factor limiting the accuracy of the approach.

The proposed technique for vertical deflection predictions is based on three publicly available data sets: (1) EGM2008, (2) DTM2006.0 and (3) SRTM elevation data. This allows replication of the approach for improving the accuracy of EGM2008 vertical deflection predictions in regions with a rough topography or for improved validation of EGM2008 and future high-degree spherical harmonic models by means of independent ground truth data.

**Keywords** vertical deflection · spherical harmonic synthesis · Earth gravitational model EGM2008 · residual terrain model (RTM)

## 1 Introduction

Recently a significant advancement was made in high-degree spherical harmonic modelling of Earth's gravity field with the release of the new Earth Gravitational Model 2008 (EGM2008) computed by the U.S. National Geospatial-Intelligence Agency (NGA) EGM Development Team

(Pavlis et al. 2008). EGM2008 is complete to degree and order 2159 with additional spherical harmonic coefficients up to degree 2190 and order 2159. As such, it allows to compute the disturbing potential $T$ and a number of gravity field related quantities, such as height anomalies $\zeta$, gravity anomalies $\Delta g$ and vertical deflections $(\xi, \eta)$ to a spatial resolution of about 5 arc minutes, corresponding to approximately 9 km in latitude.

It is clear that the high-frequency features of Earth's gravity field with wavelengths smaller than 5 arc minutes are not represented by EGM2008 because of the truncation of the spherical harmonic expansion at degree 2160. This produces a signal omission error (e.g. Torge 2001, p. 273) with amplitudes estimated to be on the order of a few arc seconds in the case of vertical deflections (Torge 1981).

Astrogeodetic vertical deflections, obtained from astronomical observations (e.g. Hirt and Seeber 2008; Torge 2001) contain the full spectral signal. They can be used to estimate the signal omission error by means of a comparison with vertical deflections from spherical harmonic synthesis.

Jekeli (1999) compared a number of astrogeodetic vertical deflections with vertical deflections derived from the spherical harmonic model EGM96 (Lemoine et al. 1998) and revealed larger differences in mountainous areas than in low-elevated terrain. This result is related to the fact that the topography generates a considerable portion of the vertical deflection signal (Forsberg and Tscherning 1981). Therefore, for vertical deflections a larger omission error is generally to be expected in mountainous areas than in low-elevated terrain.

Gravity field modelling often takes advantage of the strong correlation between the topography and the short wavelength parts of the gravity field by means of digital terrain model (DTM) data (e.g. Forsberg and Tscherning 1981; Denker 1988; Marti 1997). In particular, residual terrain model (RTM) data can be used to reconstitute a significant part of the short wavelength components

of the gravity field (e.g. Forsberg 1984) which are omitted by a truncated spherical harmonic series expansion. Generally, RTM data is constructed from detailed digital terrain model (DTM) data from which a smooth reference grid is subtracted (Forsberg 1994). The latter serves as high-pass filter and eliminates the long wavelengths from the DTM data. If the reference grid is constructed consistently with the maximum degree of the spherical harmonic model, the RTM data will augment the spherical harmonic model beyond its maximum degree. This results in an extension of the spectral content of the spherical harmonic vertical deflections and, hence, in a reduction of the omission error.

In recent time, several studies have been carried out aiming at the validation of spherical harmonic vertical deflections from EGM2008 by means of astrogeodetic deflections (e.g. Claessens et al. (2008) in Australia, Pavlis et al. (2008) in the United States of America, Huang and Véronneau (2009) in Canada), however, without modelling the signal omission error using RTM data. Also, the paper by Jekeli (1999) that thoroughly analyses vertical deflections from EGM96 does not attempt to model the signal omission error. To the knowledge of the author, no studies on the augmentation of high-degree spherical harmonic vertical deflections with RTM data are published in the recent geodetic literature by now.

The aim of the present study is to demonstrate that in mountainous areas a significant part of the omission error of vertical deflections from spherical harmonic models in general and from EGM2008 in particular can be modelled based on RTM data. This is accomplished by means of vertical deflections computed based on properly constructed RTM data (Sec. 3). A set of 223 high-precision astrogeodetic vertical deflections, collected in two test areas in the Bavarian and Swiss Alps, serves as ground truth data against which the approach is tested (Sec. 4). It is shown that the proposed technique significantly improves the accuracy of vertical deflections in mountainous areas. As such, the augmentation of EGM2008 vertical deflections with RTM data generally al-

lows an improved prediction of vertical deflections in all mountainous areas with SRTM terrain data available. In particular, the proposed approach enables a better, more expressive validation of spherical harmonic models with astrogeodetic vertical deflections.

## 2 Definitions

In view of the following sections, it is useful to define the term "vertical deflection". Following Jekeli (1999), the vertical deflection is generally defined as angle between the Earth's gravity vector and some reference direction. The direction of the Earth's gravity vector is identical with the direction of the (physical) plumb line. It is oriented with respect to the International Terrestrial Reference System (ITRS) using the astronomical coordinates $\Phi$ (astronomical latitude) and $\Lambda$ (astronomical longitude). Depending on the reference direction chosen, we distinguish between Helmert's and Molodensky's definition of the vertical deflection.

*Helmert's* definition utilizes the ellipsoidal normal as reference which is described with the geodetic coordinates $\varphi$ (geodetic latitude) and $\lambda$ (geodetic longitude), cf. Jekeli (1999):

$$
\begin{aligned}
\xi_{Hel} &= \Phi - \varphi + \tfrac{1}{2}\eta^2 \tan\varphi, \\
\eta_{Hel} &= (\Lambda - \lambda)\cos\varphi.
\end{aligned}
\tag{1}
$$

Here, third order terms are neglected and axis parallelism of the ITRS and the ellipsoid the geodetic coordinates $(\varphi, \lambda)$ refer to is assumed. Vertical deflections $(\xi, \eta)_{Hel}$ according to Helmert's definition refer to points located at the Earth's surface and are also known as surface vertical deflections. In geodetic practice, Helmert vertical deflections are an important type of vertical deflection because they can be directly determined from observation: Astrogeodetic techniques (cf. Hirt et al. 2009) are used to measure the direction of the plumb line $(\Phi, \Lambda)$ at points with geodetic coordinates $(\varphi, \lambda)$, which are known from satellite positioning, e.g. using the Global

Positioning System GPS, cf. Seeber (2003). The Helmert vertical deflection $(\xi, \eta)_{Hel}$ is often referred to as astrogeodetic vertical deflection. Typically, they are smaller than $10''$ in low-elevated terrain. In medium-elevated and mountainous terrain, Helmert vertical deflections often amount to 20-30$''$, but rarely exceed an order of $1'$ (Torge 2001).

*Molodensky* vertical deflections use the plumb line of the normal gravity field instead of the ellipsoidal normal as reference direction (Torge 2001, p. 218). The difference among Molodensky and Helmert vertical deflections is caused by the curvature of the normal plumb line which, however, only affects the North-South component $\xi$ (cf. Jekeli 1999, Heiskanen and Moritz 1967):

$$\delta\xi^{NC} = 0''17 \cdot h[\mathrm{km}] \cdot \sin 2\varphi \tag{2}$$

where $h$ is the ellipsoidal height of the point in [km] and $\varphi$ the geodetic latitude. As a consequence of Eq. 2, amplitudes of about $0''5$ may be reached for $\delta\xi^{NC}$ in mountainous areas (heights of 3 km) whereas the effect almost disappears in flat terrain. The relation among Molodensky and Helmert vertical deflections reads (Heiskanen and Moritz 1967):

$$\xi_{Hel} = \xi_{Mol} + \delta\xi^{NC},$$
$$\eta_{Hel} = \eta_{Mol}. \tag{3}$$

Due to the rotational symmetry of the normal gravity field, there is no difference among the East-West component $\eta$ in both definitions. Other definitions, like the Pizetti definition of the vertical deflection (cf. Torge 2001) are not relevant for this study.

## 3 Methodology

### 3.1 Vertical deflections from spherical harmonic synthesis

A spherical harmonic model of the Earth's global gravity field, such as EGM2008, comprises a set of fully-normalized spherical harmonic coefficients $\overline{C}_{nm}, \overline{S}_{nm}$ with $n$ denoting the degree and

$m$ the order of the coefficients. This coefficient set is used for the computation of the disturbing potential $T$ using the spherical harmonic series expansion (Torge 2001, p. 215, Smith 1998):

$$T(r, \theta, \lambda) = \frac{GM}{r} \sum_{n=2}^{n_{max}} \left(\frac{a}{r}\right)^n \sum_{m=0}^{n} (\overline{\delta C}_{nm} \cos m\lambda +$$

$$\overline{S}_{nm} \sin m\lambda) \overline{P}_{nm}(\cos \theta). \tag{4}$$

The parameters $GM$ (geocentric gravitational constant) and $a$ (semi-major axis of the geocentric reference ellipsoid) are the model-specific scaling parameters which are provided along with the set of harmonic coefficients. $\overline{P}_{nm}(\cos \theta)$ denotes the fully-normalized associated Legendre functions (cf. Torge 2001, p. 71). The term $\overline{\delta C}_{nm}$ expresses that a series expansion of the normal gravity field (mostly up to degree 10) is subtracted from the model's even zonal harmonics $\overline{C}_{nm}$ (cf. Smith 1998). The variable $n_{max}$ indicates the maximum spherical harmonic degree of the series expansion.

The spherical polar coordinates of the point $P$ under evaluation ($r$ distance of $P$ from the geocentre, $\theta$ geocentric co-latitude and $\lambda$ geodetic longitude) are obtained from (ellipsoidal) geodetic coordinates ($\varphi$ geodetic latitude, $\lambda$ geodetic longitude, $h$ ellipsoidal height) via a conversion to global Cartesian coordinates $(X, Y, Z)$ (cf. Torge 2001, p. 94 and p. 100; Jekeli 2006, p. 2-41).

Vertical deflections $(\xi, \eta)_{Mol}$ are the partial derivatives of the disturbing potential $T$ [Eq. (4)] in direction of geocentric latitude $\bar{\varphi}$ and longitude $\lambda$ (Torge 2001, p. 258, Roland 2005, p. 7):

$$\begin{aligned} \xi_{Mol} &= -\frac{1}{\gamma r} \frac{\partial T}{\partial \bar{\varphi}}, \\ \eta_{Mol} &= -\frac{1}{\gamma r \cos \theta} \frac{\partial T}{\partial \lambda}. \end{aligned} \tag{5}$$

The partial derivatives $\frac{\partial T}{\partial \bar{\varphi}}$ and $\frac{\partial T}{\partial \lambda}$ may be computed numerically or analytically; see e.g. Wenzel (1985) or Wolf (2007) for the analytical expressions.

The $(\xi, \eta)_{Mol}$ values are also known as "gravimetric vertical deflection" in the literature (cf. Jekeli 1999). They implicitly refer to the curved normal plumb line because of the subtracted normal gravity field the series expansion for the disturbing potential is based on. Eq. (5) yields vertical deflections according to the *Molodensky* definition, however in *spherical* approximation. This is because the partial derivatives in Eq. (5) refer to the plane which is orthogonal to the direction of $r$ and not to the direction of the ellipsoidal normal $h$. For the computation of the correction term yielding Molodensky vertical deflections in *ellipsoidal approximation*, the reader is referred to Jekeli (1999), Eq. 30 ibid. The differences between Molodensky vertical deflections in spherical and ellipsoidal approximation are on the order of a few $0''.01$ for the North-South component $\xi_{Mol}$, whereas the East-West-component $\eta_{Mol}$ is unaffected by the spherical approximation (cf. Jekeli 1999). The correction of the spherical approximation is not further treated in this paper because this effect is small compared to the residuals between astrogeodetic deflections and spherical harmonic deflections corrected for the omission error from RTM data (cf. Sec. 4). This also holds for further second-order effects (e.g. tidal correction of vertical deflections) which are omitted here due to their small amplitudes (for details on these effects see Jekeli 1999).

3.2 Vertical deflections from topographic data

In gravity field modelling, digital terrain model (DTM) data is a commonly used data source which provides information on the short-wavelength constituents of the gravity field (e.g. Forsberg and Tscherning 1981; Denker 1988; Marti 1997). The term *residual terrain model* (RTM) denotes a DTM from which a smooth reference surface (i.e. a low-pass filtered DTM) is subtracted (Forsberg 1994). As such, the RTM represents only the high-frequency features of the terrain (cf. Forsberg 1984).

By now, a variety of DTM data sets with different resolution and accuracy is used in gravity field modelling, e.g. GLOBE, GTOPO, SRTM as well as national elevation data sets. The present study is deliberately carried out using the globally and publicly available SRTM elevation data because the use of which allows applying the proposed method without any restrictions of accessibility most of the national data sets are affected by.

### 3.2.1 SRTM elevation data

On most of the land surfaces between latitudes $60°$ North and $56°$ South, digital elevation data $H_{SRTM}$ is available from the Shuttle Radar Topography Mission (SRTM) with a resolution of 90 m (3") (cf. Werner 2001). The vertical accuracy of SRTM elevation was analysed by several authors, e.g. Denker (2004); Marti (2004); Jakobsen (2005). The accuracy estimates (1 sigma) obtained from comparisons with national elevation data sets range between 4 m and 6 m for low-elevated terrain and go up to 11 m to 14 m for mountainous areas.

While the original release of SRTM elevation data in 2003 contained numerous data gaps (holes), particularly in mountainous areas or over water areas (cf. Denker 2004), today post-processed SRTM releases are available where the gaps have been filled using interpolation methods (cf. Reuter et al. 2007). This study uses the latest post-processed SRTM release (V4.1) by the Consortium for Spatial Information of the Consultative Group for International Agricultural Research (CGIAR-CSI), cf. Jarvis et al. (2008). The V4.1 SRTM elevation data is hole-filled based on the application of a range of different interpolation methods (e.g. kriging, spline interpolation, inverse distance weighting and interpolation using auxiliary DEM data) which were applied depending on the terrain type (e.g. low-elevation areas, mountainous areas). Importantly, the release V4.1 features considerably better quality in many mountainous areas, such as the European Alps. In particular, many summits were reconstructed from auxiliary DEM data sets which is a very sig-

nificant advancement over previous SRTM releases. For a detailed description of the hole-filling algorithms see Reuter et al. (2007).

It is fully acknowledged that, despite the clear improvements over earlier versions, the SRTM data release V4.1 is not a perfect representation of the terrain surface, e.g. isolated errors on the order of 100 m can still be found in mountainous areas. What is more, heights may be systematically too high in forest regions due to the fact that SRTM is a surface model and not a terrain model (cf. Marti 2004). Nevertheless, the SRTM release V4.1 can be used with success to significantly improve vertical deflections from spherical harmonic synthesis (see results in Sec. 4).

*3.2.2 Construction of the RTM*

Forsberg (1994) suggests two different ways to define the reference surface of the RTM. The long-wavelength reference can be obtained from a spherical harmonic series expansion of the global topography. Alternatively, a smooth reference surface can be constructed by applying the moving average (MA) operator on the DTM. Importantly, the associated spherical harmonic degree of the reference surface should agree with the maximum spherical harmonic degree $n_{max}$ of the Molodensky vertical deflections [Eq. (5)]. Then, the RTM data is capable of providing information on the omitted short-wavelength parts of the Molodensky vertical deflections. In this study, both variants of constructing the reference surface of RTM data are tested.

As high-degree spherical harmonic series expansion of the Earth's topography, the digital terrain model DTM2006.0 is used. DTM2006.0, computed by the EGM2008 development team based on the SRTM global elevation data set and some other data sources described in Pavlis et al. (2007), is complete to degree and order 2190 (approx. 5' resolution). The model DTM2006.0 consists of a set of 2,401,336 fully-normalized coefficients $\overline{HC}_{nm}$, $\overline{HS}_{nm}$ which are transformed to heights of the topography using the series expansion (EGM-Team 2008):

$$H_{ref}^{DTM2006.0}(\theta, \lambda) = \sum_{n=0}^{n_{max}} \sum_{m=0}^{n} (\overline{HC}_{nm} \cos m\lambda +$$

$$\overline{HS}_{nm} \sin m\lambda) \overline{P}_{nm}(\cos \theta) \tag{6}$$

with $\theta$ geocentric co-latitude, $\lambda$ longitude and $\overline{P}_{nm}(\cos\theta)$ fully-normalized associated Legendre functions. DTM2006.0 is a consistent supplement of the Earth's gravitational model EGM2008.

As a second approach, a smooth reference surface is constructed using the moving average operator. Moving-averaged heights $H_{ref}^{MA}$ can be computed from

$$H_{ref}^{MA}(k, l) = \frac{1}{(2n+1)(2n+1)} \sum_{i=-n}^{i=n} \sum_{j=-n}^{j=n} H(k+i, l+j) \tag{7}$$

where $H$ is a matrix containing the DTM data, $(k, l)$ is the pair of indices denoting the computation point. The parameter $n$ can be easily determined from the width $w$ of the filter window and the DTM resolution $\Delta x$:

$$n = \text{int}(\frac{w}{2\Delta x}). \tag{8}$$

Eq. 7 uses a square-shaped window centred to the computation point. In order to construct the moving-averaged reference surface in agreement with the maximum spherical harmonic degree $n_{max}$ of the Molodensky vertical deflections (Sec. 3.1), the window width $w$ is adapted to the spatial resolution of the spherical harmonic expansion (after Torge 2001, p. 74):

$$w = \frac{180 \deg}{n_{max}}. \tag{9}$$

In the case of EGM2008, the maximum degree $n_{max}$ of 2160 implies a window width $w$ of 5 arc minutes.

*3.2.3 RTM vertical deflections*

A digital elevation grid (this can be a DTM or RTM) offers a discretization of the topography by means of elementary geometric bodies, e.g. rectangular prisms or tessoroids, for which the gravitational potential $V$ can be computed (e.g. Tsoulis 1999; Nagy et al. 2000; Heck and Seitz 2007). The horizontal derivatives $V_x$ and $V_y$ of the gravitational potential of such an elementary body represent its contribution to vertical deflections $\xi$ and $\eta$ (Nagy et al. 2000). In case of the frequently used right rectangular prism with constant density $\rho$, the equations for the computation of $V_x$ and $V_y$ in flat Earth approximation read (Nagy et al. 2000, 2002):

$$V_x = G\rho \left|\left|\left| y\ln(z+r) + z\ln(y+r) - x\tan^{-1}\frac{yz}{xr} \right.\right.\right.{\left.\right|}_{x_1}^{x_2}{\left.\right|}_{y_1}^{y_2}{\left.\right|}_{z_1}^{z_2},$$

$$\tag{10}$$

$$V_y = G\rho \left|\left|\left| z\ln(x+r) + x\ln(z+r) - y\tan^{-1}\frac{xz}{yr} \right.\right.\right.{\left.\right|}_{x_1}^{x_2}{\left.\right|}_{y_1}^{y_2}{\left.\right|}_{z_1}^{z_2}$$

where $G$ is the gravitational constant and $r$ is the distance of the points $(x, y, z)$ from the origin of the coordinate system. The limits $(x_1, x_2, y_1, y_2, z_1, z_2)$ describe the boundaries of the prism faces with respect to the computation point (cf. Nagy et al. 2000). For each single prism, the evaluation of Eq. 10 requires substituting the variables $(x, y, z)$ by the eight corner coordinates of the prism $(x_1, y_1, z_1)$ , $(x_1, y_1, z_2)$,...,$(x_2, y_2, z_2)$, resulting in a total of 24 terms for $V_x$ and $V_y$, respectively. In the literature, alternative equations for the computation of $V_x$, $V_y$ are found that use arsinh- instead of ln-terms (cf. Tsoulis 1999; Flury 2002). Eq. 10 is based on a planar approximation (Nagy et al. 2000), however, the effect of Earth curvature may be taken into account by a vertical shift of the prism as a function of the distance between prism and computation point (cf. Forsberg 1984, p. 111).

Eq. 10 assumes the z-axis of the $(x, y, z)$ Cartesian coordinate system representing the RTM elevation data. Importantly, the prism's height $z_2 - z_1$ must be equal to the residual elevation $z_{RTM}$ = $H_{SRTM} - H_{ref}$. In the present study, we evaluate Eq. 10 using $z_1 = 0$ and $z_2 = z_{RTM}$.

The contribution of the complete residual terrain to vertical deflections is obtained by summation (numerical integration) of the horizontal derivatives of the gravitational potential of all prisms a digital RTM elevation grid consists of, and by division with the normal gravity $\gamma$ (after Nagy et al. 2000):

$$\xi^{RTM} = -\frac{1}{\gamma} \sum V_x,$$
$$\eta^{RTM} = -\frac{1}{\gamma} \sum V_y. \tag{11}$$

The values $(\xi, \eta)^{RTM}$ are denoted *RTM vertical deflections* as they are the contribution of the RTM data on the vertical deflections. RTM vertical deflections are a measure of the omission error of vertical deflections as obtained from a spherical harmonic series extension of the Earth's gravity field. Because RTM vertical deflections $(\xi, \eta)^{RTM}$ are mostly on the order of some arc seconds and scarcely exceed $10''$ (cf. Sec. 4), it is usually sufficient to introduce a coarse value of 9.80 m s$^{-2}$ for $\gamma$ in practical computations.

In other studies, the original, i.e. unfiltered, DTM heights and not residual RTM elevations were used for computing *topographic vertical deflections*, i.e. the contribution of the topography above the geoid to vertical deflections (e.g. Heitz 1968; Hirt and Flury 2008; Hirt et al. 2008). The difference among RTM vertical deflections (used here) and topographic vertical deflections (as used in the mentioned studies) is the spectral content: RTM vertical deflections exclusively contain high-frequency signals with wavelengths shorter than the wavelength implied by the maximum spherical harmonic degree $n_{max}$ of the RTM reference surface; topographic vertical deflections as used e.g. in Hirt and Flury (2008) contain both short and medium wavelengths as generated by the (unfiltered) topography.

*3.2.4 Role of the DTM grid extension*

It is a well-known advantage of RTM computations that the numerical integration of gravitational effects (Eqs. 10, 11) need only to be carried out to some certain distance because of the oscillating positive and negative RTM elevations (cf. Forsberg 1984, p. 38; Forsberg 1994). This is demonstrated by test computations of $(\xi, \eta)^{RTM}$ values using a set of different integration radii. For the station "Sion" located in the Swiss Alps, Fig. 1 exemplarily shows the RTM vertical deflections $(\xi, \eta)^{RTM}$ as a function of the maximum integration distance, ranging from 1 km to 80 km. It is seen that small integration radii around 10-20 km are not necessarily sufficient in order to obtain stable $(\xi, \eta)^{RTM}$ estimates. At the selected station, the RTM vertical deflections sufficiently converge for radii of about 40 km and larger. Further analyses of RTM vertical deflections of other stations in the European Alps (cf. Sec. 4.1) corroborated this result, i.e. most of the RTM vertical deflections computed with radii of 40 km to 50 km differed by less than $0''05$ from the numerical integration results using a radius of 80 km as reference. These tests provide some evidence that considering all prisms within a distance of 50 km from the computation point yields reasonably stable values of RTM vertical deflections.

3.3 Combination

Helmert vertical deflections $(\xi, \eta)^{EGM2008}_{Hel}$ are computed from EGM2008 spherical harmonic coefficients up to degree 2160 using Eqs. (4), (5), and by correcting the curvature of the normal plumb line using Eqs. (2), (3). The high-degree spectral power of degrees 2161 and beyond is delivered by RTM vertical deflections $(\xi, \eta)^{RTM}$, cf. Eqs. (10) and (11). A simple spectral combination yields

$$
\begin{aligned}
\xi^{EGM/RTM}_{Hel} &= \xi^{EGM}_{Mol} + \delta\xi^{NC} + \xi^{RTM}, \\
\eta^{EGM/RTM}_{Hel} &= \eta^{EGM}_{Mol} + \eta^{RTM}.
\end{aligned}
\tag{12}
$$

In the sequel, we denote this combination *EGM/RTM vertical deflections* $(\xi, \eta)_{Hel}^{EGM/RTM}$. These correspond to Helmert's definition of vertical deflections, in that, they are comparable to observed surface vertical deflections. The $(\xi, \eta)_{Hel}^{EGM/RTM}$ values not only possess spectral energy in the long- and medium wavelengths (degrees up to 2160) but also on the short scales well beyond spherical harmonic degree 2160. This is demonstrated in the next section.

## 4 Testing the approach

### 4.1 Test areas with ground truth data

In order to test the proposed approach for the prediction of vertical deflections, mountainous test areas in the European Alps were selected with high-precision sets of astrogeodetic vertical deflections $(\xi, \eta)^{astro}$ available. All astrogeodetic deflections used in this study were determined in the years 2003 to 2005 from star observations using the Hannover Digital Zenith Camera System (e.g. Hirt 2004, Hirt et al. 2009). The astrogeodetic vertical deflections correspond to the Helmert definition given in Sec. 2. Because of an accuracy level of $0''08 - 0''1$ (cf. Hirt and Seeber 2008, Hirt and Flury 2008), these observed data sets are considered to provide the reference (ground truth) for the comparison with predicted values of vertical deflections from EGM2008 and RTM data (Eq. 12).

In the *Ester Mountains* (Estergebirge), located in the Bavarian Alps, Germany, a total of 188 stations with vertical deflections from digital zenith camera measurements is available, cf. Fig. 2). 103 out of the 188 stations are located in the *Isar Valley*, they form a dense traverse of about 23 km length (cf. Hirt and Flury 2008). Another 85 still unpublished stations are available at scattered locations in and around the Ester mountains, extending over an area of approximately 15 km x 20 km. The heights of the 188 benchmarks range from 700 m to about 1500 m. The selected test area is part of the geodetic testing net work "Estergebirge" of the Technical University Munich and

subject of numerous studies of terrain effects and gravity field quantities such as gravity anomalies, height anomalies and GPS/levelling (cf. Tsoulis 2001; Flury 2002, 2006; Hirt et al. 2007; Hirt and Flury 2008; Flury et al. 2009).

Additionally, we use a set of 35 astrogeodetic vertical deflections in the test area *Switzerland* (Hirt 2004; Müller et al. 2004). Fig. 3 shows that these benchmarks are almost randomly distributed over complete Switzerland. The elevations of the Swiss astrogeodetic benchmarks cover a range from 300 m to 2800 m. Most of the stations are located along roads in Alpine valleys, however, 8 stations are located at summit roads with heights of 1500 m and above. The descriptive statistics of the sets of astrogeodetic vertical deflections $(\xi, \eta)^{astro}$ is given in the top part of Tab. 1.

## 4.2 Computation of EGM/RTM vertical deflections

According to the procedure described in Sec. 3.1, EGM2008 vertical deflections $(\xi, \eta)_{Mol}^{EGM}$ were computed at the geodetic positions $(\varphi, \lambda, h)$ of all 223 stations with observed astrogeodetic data available. The spherical harmonic synthesis of the EGM2008 coefficients was done for the range of spectral degrees 2 to 2160 using the synthesis software *harmonic_synth* by the EGM2008 development team.

Correcting the curvature of the normal plumb line [Eqs. (2), (3)] yielded Helmert vertical deflections $(\xi, \eta)_{Hel}^{EGM}$. Subsequently, the subscript $_{Hel}$ is neglected as all further comparisons are exclusively made among Helmert-type vertical deflections. The middle section of Tab. 1 shows the descriptive statistics of the EGM2008-based (Helmert) vertical deflections.

RTM vertical deflections were determined based on the 90 m V4.1 SRTM elevation data set, cf. Sec. 3.2. As reference surface, we used in a first computation elevations $H_{ref}^{DTM2006.0}$ from the spherical harmonic elevation model DTM2006.0 with a maximum spherical degree $n_{max}$ of 2160, yielding RTM vertical deflections $(\xi, \eta)_{DTM2006.0}^{RTM}$. A second computation applied a moving-

averaged (MA) SRTM surface $H_{ref}^{MA}$ with an equivalent window width $w$ of 5 arc minutes for the $(\xi, \eta)_{MA}^{RTM}$ calculation. This allows the evaluation of how the RTM reference surface should be constructed. In all cases, numerical integration was carried out within a circular window of 50 km radius (centred to the computation point), the dimension of which was found to be completely sufficient (cf. 3.2.4). All computations are based on a standard rock density $\rho$ of 2670 kg/m$^3$ (cf. Eq. 10). The descriptive statistics of the RTM vertical deflections $(\xi, \eta)_{DTM2006.0}^{RTM}$ is listed in the bottom part of Tab. 1.

An impression of the elevation grids generated for the computation of $(\xi, \eta)_{DTM2006.0}^{RTM}$ vertical deflections is given in Fig. 4 for the station "Grosse Scheidegg" in the Central Alps of Switzerland. Fig. 4a shows the SRTM elevation data, illustrating the roughness of topography in the vicinity of the benchmark. The DTM2006.0 spherical harmonic elevation model (Fig. 4b) shows the spectral features of up to degree 2160 for the same area. The reference grid from DTM2006.0 is subtracted from the 90 m SRTM elevations, yielding fairly balanced positive and negative RTM elevations which are visible in Fig. 4c. The latter is used as input data for the computation of RTM vertical deflections $(\xi, \eta)_{DTM2006.0}^{RTM}$ with Eqs. (10) and (11).

## 4.3 Comparisons and Analyses

The comparison among the vertical deflections $(\xi, \eta)^{EGM}$ from EGM2008 and the ground truth astrogeodetic deflections $(\xi, \eta)^{astro}$ at our 223 benchmarks reveals discrepancies of up to 15″ for $\xi$ and approximately 9″ for $\eta$, respectively (see descriptive statistics in Tab. 2). The root mean square (RMS) of the differences is found to be around 3″5 for $\xi$ and somewhat lower for the component $\eta$ (3″2). These values mainly reflect the signal omission of EGM2008 on the short scales (structures below 5′), EGM2008 model errors, and, to a minor extent, also noise of the astrogeodetic observations.

The differences between astrogeodetic vertical deflections $(\xi, \eta)^{astro}$ and the EGM/RTM vertical deflections $(\xi, \eta)^{EGM/RTM}_{DTM2006.0}$ (based on the RTM with DTM2006.0 as reference) are listed in Tab. 3. It is seen that the maximum discrepancies among both data sets decrease from $15''$ to $3''\!.6$. The RMS values of the differences are considerably improved from $3''\!.50$ ($\xi$) and $3''\!.21$ ($\eta$) to $0''\!.80$ ($\xi$) and $0''\!.72$ ($\eta$), respectively. This represents a significant improvement of more than 75 %. The improved agreement is also illustrated in Fig. 5, showing the distribution of residual differences for EGM2008 only vertical deflections (top) and EGM/RTM vertical deflections (middle), all with respect to the astrogeodetic observations. Tab. 3 lists the detailed results for the different test areas Ester Mountains, Isar Valley and Switzerland. It is seen that for the improvement rates of the RMS values, irrespective of the area and vertical deflection component, always reach or exceed a level of about 65%. These results are considered to be a clear manifestation that the proposed augmentation of vertical deflections from spherical harmonic synthesis with RTM based vertical deflections enhances the spectral power to the short scales of the spectrum. The differences among our astrogeodetic deflections $(\xi, \eta)^{astro}$ and EGM/RTM deflections $(\xi, \eta)^{EGM/RTM}$ are not correlated with the station height which is seen in Fig. 7.

An experimental computation using a maximum spherical degree $n_{max}$ of 2190 for the computation of EGM/RTM vertical deflections $(\xi, \eta)^{EGM/RTM}$ yielded similar RMS values ($0''\!.79$ for $\xi$ and $0''\!.78$ for $\eta$, respectively) as previously seen with degree 2160.

A detailed analysis of the 103 stations arranged in a traverse in the Isar Valley (cf. Fig. 6) provides some interesting insight into EGM/RTM vertical deflections. The upper part of Fig. 6 shows the differences between astrogeodetic and EGM2008 vertical deflections (without any RTM data). The RTM vertical deflections $(\xi, \eta)^{RTM}$, representing the omitted gravity field signal generated by the topography at short scales below 5 arc minutes, are depicted in the middle part of Fig. 6. The strong correlation between these two data sets demonstrates that a large part of the discrep-

ancies among EGM2008 only vertical deflections and the astrogeodetic ground truth results from signal omission. Augmenting the EGM2008 vertical deflections $(\xi, \eta)^{EGM}$ with RTM vertical deflections $(\xi, \eta)^{RTM}$ yields to a very good agreement with the astrogeodetic data set (bottom part of Fig. 6). The residual wave-like features with amplitudes on the order of $0\rlap{.}''5$-$1\rlap{.}''0$ are due to local density anomalies (e.g. Pleistocene valley fillings or lakes), cf. Flury (2002); Hirt and Flury (2008). Similarly correlated residuals are of course to be expected in all cases where the density of the real topography deviates from the RTM standard rock density of 2670 kg/m$^3$. It should be noted that the residual signals feature very low noise of about $0\rlap{.}''1$-$0\rlap{.}''2$, which indicates the good quality of the EGM/RTM vertical deflections on the one hand and those of the astrogeodetic deflections on the other hand.

A further comparison is drawn among the sets of astrogeodetic vertical deflections $(\xi, \eta)^{astro}$ and EGM/RTM vertical deflections $(\xi, \eta)_{MA}^{EGM/RTM}$ computed based on the RTM elevations with a MA reference surface. Tab. 4 shows that RMS values from differences of about $2\rlap{.}''1$ ($\xi$) and $1\rlap{.}''5$ ($\eta$) are obtained and that the improvement rates (as compared with the EGM2008 only RMS values listed in Tab. 2) are 39% ($\xi$) and 54% ($\eta$). These percentages are much lower than previously obtained with RTM vertical deflections that are based on a spherical harmonic reference surface (cf. histogram in Fig. 5). These results suggest that the RTM data should be constructed based on a spherical harmonic reference surface, such as DTM2006.0, which allows combining RTM vertical deflections with EGM2008 vertical deflections in a consistent way.

## 5 Discussion and conclusions

A new approach for the improved prediction of vertical deflections in rugged terrain was introduced and successfully tested in this study. EGM2008 vertical deflections provide spectral information of the Earth's gravitational field of up to spherical harmonic degree of 2160 with all gravity

field features at scales smaller than 5 arc minutes omitted. RTM vertical deflections, as obtained from SRTM height data referred to the DTM2006.0 spherical harmonic elevation surface are capable of reconstituting a significant part of the EGM2008 omission error. This was demonstrated by means of a comparison at 223 benchmarks in the Bavarian Alps and Switzerland with high-precision astrogeodetic vertical deflections available. The accuracy of EGM2008 vertical deflections augmented by RTM data was found to be on the order of $0''\!.8$ which is a clear improvement over those obtained from EGM2008 only vertical deflections (RMS values of about $3''\!.5$). Density anomalies of the real topography with respect to the density $\rho$ of the RTM model topography are a limiting factor of the proposed approach. A further improvement of the RTM modelling is to be expected if detailed knowledge on the geometry of density anomalies is available (e.g. Marti 1997; Flury 2002). As users often do not have access to detailed information on the density distribution, such a refined RTM modelling was not attempted in the present study.

Other than in mountainous terrain, RTM vertical deflections in low-elevated terrain are not expected to yield similarly high improvement rates. This is because RTM elevations, and hence, RTM vertical deflections are small in less-elevated areas and, additionally, are more affected by SRTM model errors in a relative sense.

There are two main applications related to improving EGM2008 vertical deflections with RTM data in medium-elevated and rugged terrain.

First, the method allows us to predict vertical deflections in mountainous areas with SRTM elevations available *more accurate* than using the EGM2008 model alone. This is because the signal omission error, which may be significant in the mountains (on the level of $3''$ RMS, as shown in this study for our test areas) can be greatly reduced by using RTM vertical deflections. As the attainable accuracy essentially depends on the EGM2008 commission error (i.e. the uncertainties related to the model coefficients, cf. Pavlis et al. 2008), and on local density anomalies (which

are not modelled here), it is, however, not possible to generally quantify the gain in accuracy. Nevertheless, an improvement in accuracy is to be expected in mountainous areas in comparison to EGM2008 only vertical deflections. The prediction of vertical deflections may be of interest e.g. for the reduction of terrestrial measurements (cf. Featherstone and Rüeger 2000), unless no precise astrogeodetic observations (e.g. Hirt and Seeber 2008) or vertical deflections based on national geoid models (e.g. Torge 2001, p. 291) are available. Importantly, the prediction of vertical deflections from spherical harmonic models and residual terrain model data only requires publicly available data sets: (1) EGM2008, (2) DTM2006.0 and (3) SRTM elevation data. Therefore, the proposed method can be easily replicated in other areas.

Second, the reduction of the EGM2008 omission error by means of RTM vertical deflections in mountainous areas allows advanced validation of the EGM2008 spherical harmonic model (and future high-degree models), as compared to the validation results published so far (cf. Sec. 1). This is because a large portion of the residual differences between EGM2008 and astrogeodetic vertical deflections can now be modelled and corrected (in our study about 75 %). The remaining residuals are expected to reflect mainly density anomalies and EGM2008 commission errors. It is intended to use further sets of astrogeodetic vertical deflections from zenith camera observations (e.g. Bürki 1989; Bürki et al. 2004; Somieski et al. 2007; Somieski 2008; Hirt et al. 2008; Hirt et al. 2009) for such a refined validation of EGM2008.

# References

Bürki B (1989)  Integrale Schwerefeldbestimmung in der Ivrea-Zone und deren geophysikalische Interpretation. Geodätisch-geophysikalische Arbeiten in der Schweiz, Nr. 40. Schweizerische Geodätische Kommission

Bürki B, Müller A, Kahle H-G (2004)  DIADEM: The New Digital Astronomical Deflection Measuring System for High-precision Measurements of Deflections of the Vertical at ETH Zurich. Electronic Proc. IAG GGSM2004 Meeting in Porto, Portugal. Published also in: CHGeoid 2003, Report 03-33 A (ed. U. Marti et al), Bundesamt für Landestopographie (swisstopo), Wabern, Schweiz

Claessens SJ, Featherstone WE, Anjasmara, IM (2008)   Is Australian data really validating EGM2008 or is EGM2008 just in/validating Australian data. In: Mertikas, S. (ed.) Gravity Geoid and Space Missions, Springer, Berlin Heidelberg New York

Denker H (1988)  Hochaufloesende regionale Schwerefeldbestimmung mit gravimetrischen und topographischen Daten. Wiss. Arb. der Fachr. Vermessungswesen der Univ. Hannover 156

Denker H (2004)  Evaluation of SRTM3 and GTOPO30 Terrain Data in Germany. GGSM 2004 IAG International Symposium Porto, Portugal (ed. C. Jekeli et al.), Springer, Heidelberg: 218-223

EGM2008-Team (2008)  Description of files related to the EGM2008 Global Gravitational Model. U.S. National Geospatial-Intelligence Agency (NGA) EGM2008 Development Team

Featherstone WE, Rüeger JM (2000)  The importance of using deviations of the vertical for the reduction of survey data to a geocentric datum. Aust Surv 45(2): 46-61

Flury J (2002)   Schwerefeldfunktionale im Gebirge - Modellierungsgenauigkeit, Messpunktdichte und Darstellungsfehler am Beispiel des Testnetzes Estergebirge. Deutsche Geodätische Kommission C 557

Flury J (2006)  Short wavelength spectral properties of gravity field quantities. J Geod 79(10-11): 624-640. DOI: 10.1007/s00190-005-0011-y

Flury J, Gerlach C, Hirt C, Schirmer U (2009)  Heights in the Bavarian Alps: Mutual Validation of GPS, Levelling, Gravimetric and Astrogeodetic Quasigeoids. In: Drewes, H. (ed.) Geodetic Reference Frames, IAG Symposia, Vol. 134, 303-308 DOI: 10.1007/978-3-642-00860-3_47

Forsberg R, Tscherning CC (1981) The Use of Height Data in Gravity Field Approximation by Collocation. Journal of Geophysical Research 86 No B9: 7843-7854

Forsberg R (1984)  A study of terrain reductions, density anomalies and geophysical inversion methods in gravity field modelling. Report 355, Department of Geodetic Science and Surveying, Ohio State University, Columbus,

USA

Forsberg R (1994) Terrain Effects in Geoid Computations. International School for the Determination and Use of the Geoid. Lecture Notes, International Geoid School (IGS), Milan, Italy

Heck B, Seitz K (2007) A comparison of the tesseroid, prism and point-mass approaches for mass reductios in gravity field modelling. J Geod 81: 121-136. doi: 10.1007/s00190-006-0094-0

Heiskanen WA, Moritz H (1967) Physical Geodesy. W.H. Freeman and Company, San Francisco

Heitz S (1968) Geoidbestimmung durch Interpolation nach kleinsten Quadraten aufgrund gemessener und interpolierter Lotabweichungen. Deutsche Geodätische Kommission C 124

Hirt C (2004) Entwicklung und Erprobung eines digitalen Zenitkamerasystems für die hochpräzise Lotabweichungsbestimmung. Wissenschaftliche Arbeiten der Fachrichtung Geodäsie und Geoinformatik an der Universität Hannover Nr. 253. URL: http://edok01.tib.uni-hannover.de/edoks/e01dh04/393223965.pdf

Hirt C, Denker H, Flury J, Lindau A, Seeber G (2007) Astrogeodetic Validation of Gravimetric Quasigeoid Models in the German Alps - First Results. Proceed. 1. Intern. Symp. of the International Gravity Field Service, Istanbul, Turkey, Harita Dergisi, Special Issue 18, 84-89

Hirt C, Feldmann-Westendorff, U, Denker H, Flury J, Jahn C-H, Lindau A, Seeber G, Voigt C (2008) Hochpräzise Bestimmung eines astrogeodätischen Quasigeoidprofils im Harz für die Validierung des Quasigeoidmodells GCG05. Zeits. f. Verm. (zfv) 133, 108-119

Hirt C, Seeber G (2008) Accuracy analysis of vertical deflection data observed with the Hannover Digital Zenith Camera System TZK2-D. J Geod 82:347-356. doi: 10.1007/s00190-007-0184-7

Hirt C, Flury J (2008) Astronomical-topographic levelling using high-precision astrogeodetic vertical deflections and digital terrain model data. J Geod 82: 231-248. doi: 10.1007/s00190-007-0173

Hirt C, Buerki B, Somieski A, Seeber G (2009) Modern determination of vertical deflections using digital zenith cameras. Journal Surveying Engineering, accepted paper

Huang J, Véronneau, M (2009) Evaluation of the GRACE-based Global Gravity Models in Canada. Newton's Bulletin No. 4, 66-72

Jakobsen K (2005) Analysis of SRTM Elevation Models. EARSeL 3D-Remote Sensing Workshop, Porto, 2005

Jarvis A, Reuter HI, Neson, A, Guevara, E (2008) Hole-filled SRTM for the globe Version 4. available from the CGIAR-SXI SRTM 90m DATAbase: http://srtm.csi.cgiar.org

Jekeli C (1999) An analysis of vertical deflections derived from high-degree spherical harmonic models. J Geod 73(1), 10-22. DOI: 10.1007/s001900050213

Jekeli C (2006) Geometric Reference Systems in Geodesy. Division of Geodesy and Geospatial Science, School of Earth Sciences, Ohio State University

Lemoine FG, Kenyon SC, Factor JK, Trimmer RG, Pavlis NK, Chinn DS, Cox CM, Klosko SM, Luthcke SB, Torrence MH, Wang YM, Williamson RG, Pavlis EC, Rapp RH, Olson TR (1998) The development of the joint NASA GSFC and the National Imagery and Mapping Agency (NIMA) geopotential model EGM96, NASA/TP-1998-206861, National Aeronautics and Space Administration, Maryland, 575 pp

Marti U (1997) Geoid der Schweiz 1997. Geodätisch-geophysikalische Arbeiten in der Schweiz Nr. 56. Schweizerische Geodätische Kommission

Marti U (2004) Comparison of SRTM data with the national DTMs of Switzerland. Paper presented at GGSM 2004 IAG International Symposium Porto, Portugal. Published by Swisstopo, Wabern, Switzerland

Müller A, Bürki B, Kahle H-G, Hirt C, Marti U (2004) First Results from New High-precision Measurements of Deflections of the Vertical in Switzerland. GGSM 2004 IAG International Symposium Porto, Portugal (ed. C. Jekeli et al.), Springer, Heidelberg, 143-148

Nagy D, Papp G, Benedek J (2000) The Gravitational Potential and its Derivatives for the Prism J Geod 74(7-8): 552-560. DOI: 10.1007/s001900000116

Nagy D, Papp G, Benedek J (2002) Erratum: Corrections to "The gravitational potential and its derivatives for the prism" J Geod 76(8), 475-475. DOI: 10.1007/s00190-002-0264-7

Pavlis NK, Holmes SA, Kenyon SC, Factor JK (2008) An Earth Gravitational Model to Degree 2160: EGM2008. Presented at the 2008 General Assembly of the European Geoscience Union, Vienna, Austrai, April 13-18, 2008

Pavlis NK, Factor JK, Holmes SA (2007) Terrain-related gravimetric quantities computed for the next EGM. Paper presented at 1. Meeting of the International Gravity Field Service, Istanbul

Reuter HI, Nelson A, Jarvis A (2007) An evaluation of void filling interpolation methods for SRTM data. Intern. Journal of Geog. Inform. Sc. 21(9), 983-1008

Roland M (2005) Untersuchungen zur Kombination terrestrischer Schweredaten und aktueller globaler Schwerefeldmodelle. Wissenschaftliche Arbeiten der Fachrichtung Geodäsie und Geoinformatik an der Universität Hannover Nr. 255

Seeber G (2003) Satellite Geodesy. Second edition, de Gruyter, Berlin, New York

Smith DA (1998) There is no such thing as "The" EGM96 geoid: Subtle points on the use of a global geopotential model. In: IGeS Bulletin No. 8, International Geoid Service, Milan, Italy, 17-28

Somieski, AE, Bürki B, Kahle H-G, Marti U, Hirt C, Tziavos IN (2007) Determination of Highly-Precise Deflections of the Vertical: Switzerland 2003/2005, Portugal 2004 and Greece 2005. In: Swiss National Report on the Geodetic Activities in the years 2003-2007, presented to the XXIV General Assembly of the IUGG in Perugia, Italy, ISBN 978-3-908440-15-4, Swiss Geodetic Commission, 47-52

Somieski AE (2008) Astrogeodetic Geoid and Isostatic Considerations in the North Aegean Sea, Greece. Diss. ETH No. 17790, ETH Zurich, Switzerland

Torge W (1981) Resultate und Probleme der Geoidbestimmung.. Wiss. Arb. der Fachr. Vermessungswesen der Univ. Hannover Nr. 100

Torge W (2001) Geodesy. 3rd Edition, de Gruyter, Berlin, New York

Tscherning CC, Rapp, RH (1974) Closed covariance expressions for gravity anomalies, geoid undulations, and deflections of the vertical implied by anomaly degree variance models. OSU Rep. 208, Columbo, Ohio

Tsoulis D (1999) Analytical and Numerical Methods in Gravity Field Modelling of Ideal and Real Masses. Deutsche Geodätische Kommission C 510

Tsoulis D (2001) Terrain correction computations for a densely sampled DTM in the Bavarian Alps. J Geod 75(5-6), 291-307. DOI: 10.1007/s001900100176

Wenzel H-G (1985) Hochauflösende Kugelfunktionsmodelle für das Gravitationspotential der Erde. Wissenschaftliche Arbeiten der Fachrichtung Vermessungswesen der Universität Hannover Nr. 137

Werner M (2001) Shuttle Radar Topography Mission (SRTM), Mission overview. Journ. Telecom. 55, 75-79

Wolf KI (2007) Kombination globaler Potentialmodelle mit terrestrischen Schweredaten für die Berechnung der zweiten Ableitungen des Gravitationspotentials in Satellitenbahnhöhe. Wissenschaftliche Arbeiten der Fachrichtung Geodäsie und Geoinformatik an der Universität Hannover Nr. 264
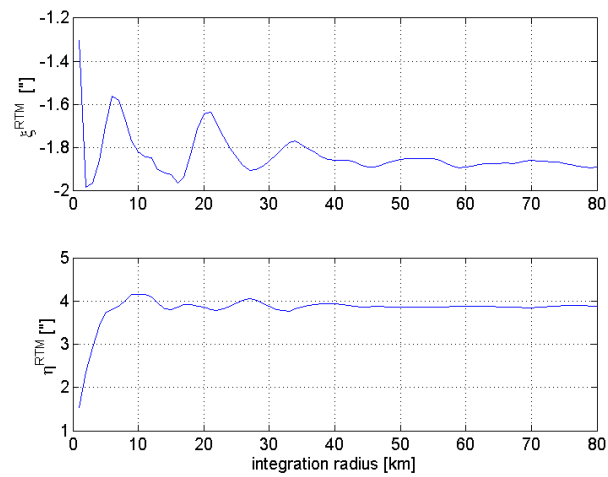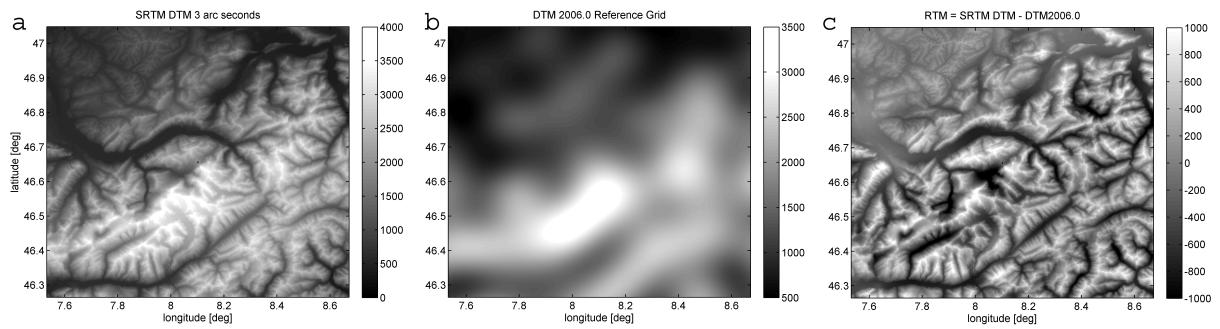
**Fig. 1** RTM vertical deflections $(\xi, \eta)^{RTM}$ for station "Sion" (located in Switzerland) as a function of the integration radius.
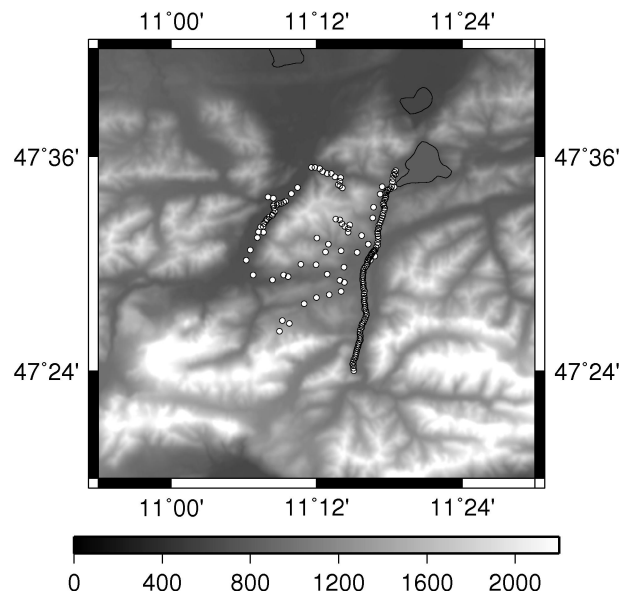


**Fig. 2** Test areas "Ester Mountains" and "Isar Valley" (Bavarian Alps, Germany) and location of 188 benchmarks with observed vertical deflections. The scalebar indicates the SRTM terrain heights, unit is [m]
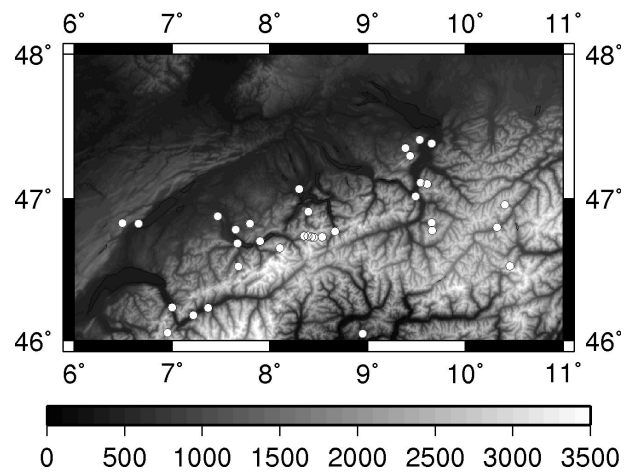
**Fig. 3** Test area "Switzerland" with 35 observed vertical deflection stations. The scalebar indicates the SRTM terrain heights, unit is [m]



**Fig. 4** Elevation grids generated for the computation of RTM vertical deflections at the station "Grosse Scheidegg" (Switzerland). (a): SRTM elevations. (b): DTM2006.0 reference grid. (c): RTM elevations obtained as difference SRTM - DTM2006.0. Units are [m].

**Table 1** Descriptive statistics of the astrogeodetic vertical deflections $(\xi, \eta)^{astro}$ (rows 1-4), the EGM2008 vertical deflections $(\xi, \eta)^{EGM}$ for spherical degrees 2 to 2160 (rows 5-8) and RTM vertical deflections $(\xi, \eta)^{RTM}_{DTM2006.0}$ from SRTM and DTM 2006.0 terrain data (rows 9-12). Units are arc seconds.

| Set | Component | Stations | $\xi$ | | | | $\eta$ | | | |
| --- | --- | --- | --- | --- | --- | --- | --- | --- | --- | --- |
| | | | Min | Max | Mean | RMS | Min | Max | Mean | RMS |
| Bavaria+Switzerland | $(\xi, \eta)^{astro}$ | 223 | -18.78 | 25.63 | 12.81 | 13.90 | -20.40 | 9.78 | 0.71 | 4.15 |
| Bavaria (Isar Valley) | $(\xi, \eta)^{astro}$ | 103 | 9.98 | 14.91 | 12.76 | 12.81 | -2.81 | 7.59 | 1.40 | 2.97 |
| Bavaria (Ester Mountains) | $(\xi, \eta)^{astro}$ | 85 | 3.25 | 24.86 | 14.73 | 15.68 | -5.68 | 9.78 | 0.89 | 3.83 |
| Switzerland | $(\xi, \eta)^{astro}$ | 35 | -18.78 | 25.63 | 8.27 | 12.27 | -20.40 | 9.67 | -1.79 | 6.95 |
| Bavaria+Switzerland | $(\xi, \eta)^{EGM}$ | 223 | -18.61 | 30.94 | 13.32 | 14.14 | -15.43 | 13.10 | -0.26 | 2.96 |
| Bavaria (Isar Valley) | $(\xi, \eta)^{EGM}$ | 103 | 10.85 | 19.17 | 14.06 | 14.26 | -1.40 | 1.08 | -0.29 | 0.91 |
| Bavaria (Ester Mountains) | $(\xi, \eta)^{EGM}$ | 85 | 10.67 | 18.68 | 14.02 | 14.21 | -0.40 | 4.97 | 0.59 | 1.23 |
| Switzerland | $(\xi, \eta)^{EGM}$ | 35 | -18.61 | 30.94 | 9.41 | 13.58 | -15.43 | 13.10 | -2.28 | 7.05 |
| Bavaria+Switzerland | $(\xi, \eta)^{RTM}_{DTM2006.0}$ | 223 | -13.16 | 6.95 | -0.17 | 3.08 | -7.85 | 7.96 | 0.54 | 2.89 |
| Bavaria (Isar Valley) | $(\xi, \eta)^{RTM}_{DTM2006.0}$ | 103 | -5.28 | 1.61 | -0.84 | 1.89 | -1.90 | 5.78 | 1.21 | 2.17 |
| Bavaria (Ester Mountains) | $(\xi, \eta)^{RTM}_{DTM2006.0}$ | 85 | -7.67 | 6.95 | 0.98 | 3.90 | -6.44 | 7.96 | -0.07 | 3.55 |
| Switzerland | $(\xi, \eta)^{RTM}_{DTM2006.0}$ | 35 | -13.16 | 6.58 | -1.02 | 3.62 | -7.85 | 5.68 | 0.06 | 2.94 |

**Table 2** Descriptive statistics of the differences among astrogeodetic and EGM2008 vertical deflections. $\Delta \xi = \xi^{astro} - \xi^{EGM}$, $\Delta \eta = \eta^{astro} - \eta^{EGM}$.

| Area | Component | Stations | Min [''] | Max [''] | Mean [''] | RMS [''] |
|------|-----------|----------|----------|----------|-----------|----------|
| Bavaria and Switzerland | $\Delta\xi$ | 223 | -15.05 | 7.03 | -0.51 | 3.50 |
| Bavaria and Switzerland | $\Delta\eta$ | 223 | -6.55 | 8.77 | 0.97 | 3.21 |
| Bavaria (Isar Valley) | $\Delta\xi$ | 103 | -6.39 | 2.36 | -1.30 | 2.62 |
| Bavaria (Isar Valley) | $\Delta\eta$ | 103 | -1.55 | 6.59 | 1.69 | 2.65 |
| Bavaria (Ester Mountains) | $\Delta\xi$ | 85 | -8.77 | 6.74 | 0.70 | 4.09 |
| Bavaria (Ester Mountains) | $\Delta\eta$ | 85 | -6.55 | 8.77 | 0.30 | 3.81 |
| Switzerland | $\Delta\xi$ | 35 | -15.05 | 7.03 | -1.14 | 4.19 |
| Switzerland | $\Delta\eta$ | 35 | -4.97 | 5.14 | 0.48 | 3.11 |

**Table 3** Descriptive statistics of the differences between astrogeodetic and EGM2008 vertical deflections augmented with RTM vertical deflections (DTM2006.0 as reference surface). $\Delta \xi = \xi_{astro} - \xi_{DTM2006.0}^{EGM/RTM}$, $\Delta \eta = \eta_{astro} - \eta_{DTM2006.0}^{EGM/RTM}$.

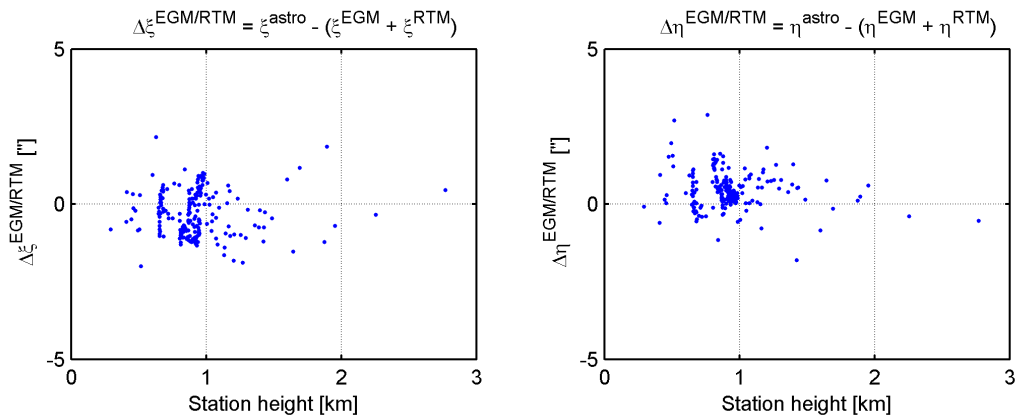| Area | Component | Stations | Min [''] | Max [''] | Mean [''] | RMS [''] | Improvement [%] |
|------|-----------|----------|----------|----------|-----------|----------|-----------------|
| Bavaria and Switzerland | $\Delta\xi$ | 223 | -2.00 | 2.16 | -0.33 | 0.80 | 77.2 |
| Bavaria and Switzerland | $\Delta\eta$ | 223 | -1.81 | 2.88 | 0.43 | 0.72 | 77.7 |
| Bavaria (Isar Valley) | $\Delta\xi$ | 103 | -1.33 | 1.00 | -0.46 | 0.85 | 67.5 |
| Bavaria (Isar Valley) | $\Delta\eta$ | 103 | 0.02 | 1.63 | 0.48 | 0.63 | 76.4 |
| Bavaria (Ester Mountains) | $\Delta\xi$ | 85 | -1.39 | 0.76 | -0.27 | 0.60 | 85.3 |
| Bavaria (Ester Mountains) | $\Delta\eta$ | 85 | -0.56 | 1.33 | 0.37 | 0.61 | 84.0 |
| Switzerland | $\Delta\xi$ | 35 | -2.00 | 2.16 | -0.12 | 1.02 | 75.6 |
| Switzerland | $\Delta\eta$ | 35 | -1.81 | 2.88 | 0.42 | 1.10 | 64.6 |
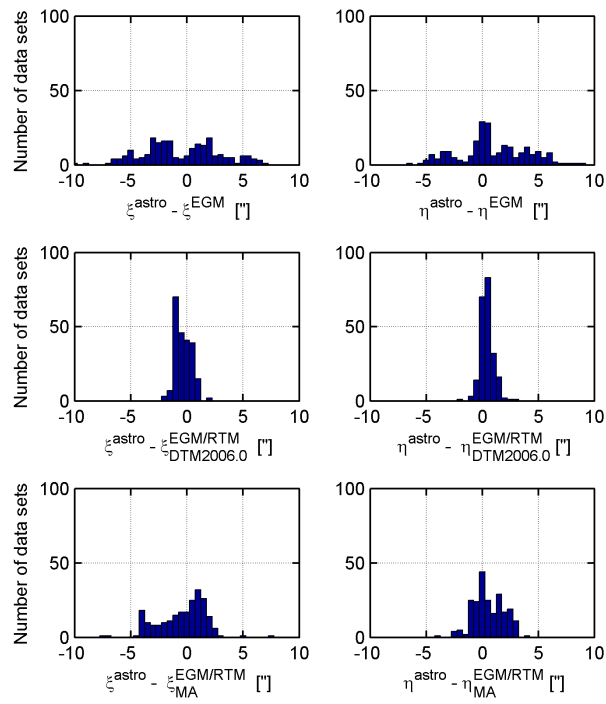
**Fig. 5** Histogram of $\xi, \eta$ differences at 223 benchmarks. Top: $(\xi, \eta)^{astro} - (\xi, \eta)^{EGM}$. Middle: $(\xi, \eta)^{astro} - (\xi, \eta)^{EGM/RTM}_{DTM2006.0}$. Bottom: $(\xi, \eta)^{astro} - (\xi, \eta)^{EGM/RTM}_{MA}$.
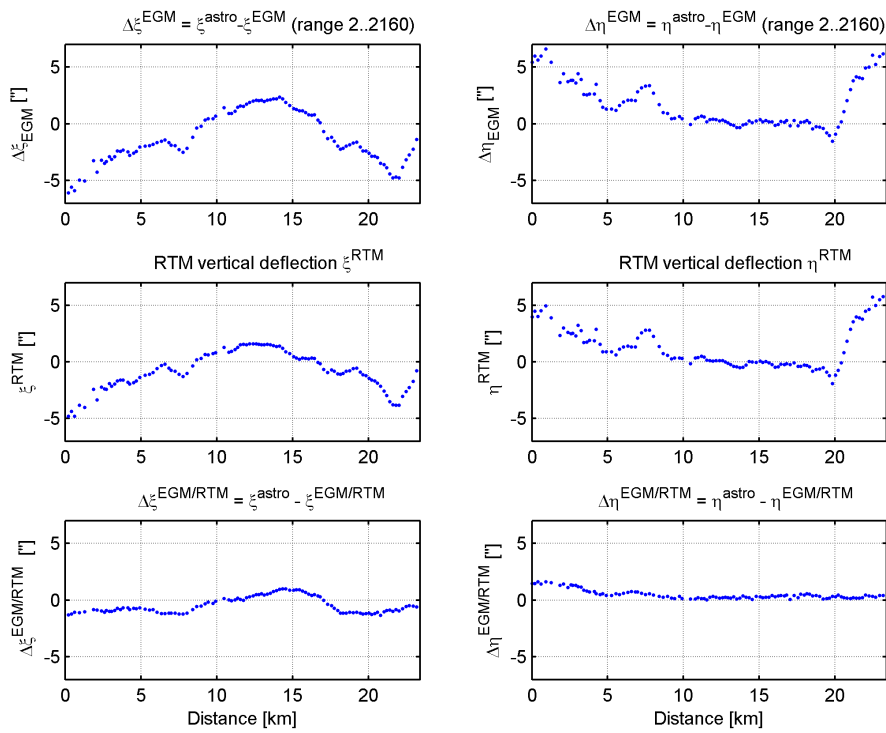
**Fig. 6** Comparisons with astrogeodetic deflections and RTM vertical deflections along a 23 km traverse in the test area Isar Valley. Top: Differences among astrogeodetic deflections $(\xi, \eta)^{astro}$ and EGM2008 only deflections $(\xi, \eta)^{EGM}$. Middle: RTM vertical deflections $(\xi, \eta)^{RTM}$ based on SRTM and DTM2006.0 as reference. Bottom: Differences among astrogeodetic deflections $(\xi, \eta)^{astro}$ and EGM2008 deflections $(\xi, \eta)^{EGM/RTM}$ augmented by RTM vertical deflections.

**Fig. 7** Differences among astrogeodetic deflections $(\xi, \eta)^{astro}$ and EGM2008/RTM $(\xi, \eta)^{EGM/RTM}$ deflections (DTM2006.0 as reference surface) as a function of the station height

**Table 4** Descriptive statistics of the differences between astrogeodetic and EGM2008 vertical deflections augmented with RTM vertical deflections (moving average MA as reference surface). $\Delta\xi = \xi_{astro} - \xi_{MA}^{EGM/RTM}$, $\Delta\eta = \eta_{astro} - \eta_{MA}^{EGM/RTM}$.

| Area | Component | Stations | Min [$''$] | Max [$''$] | Mean [$''$] | RMS [$''$] | Improvement [%] |
|---|---|---|---|---|---|---|---|
| Bavaria and Switzerland | $\Delta\xi$ | 223 | -7.66 | 7.53 | -0.39 | 2.15 | 38.7 |
| Bavaria and Switzerland | $\Delta\eta$ | 223 | -3.87 | 3.87 | 0.57 | 1.46 | 54.4 |
| Bavaria (Isar Valley) | $\Delta\xi$ | 103 | -4.25 | 2.60 | -1.04 | 2.51 | 4.2 |
| Bavaria (Isar Valley) | $\Delta\eta$ | 103 | -1.31 | 2.63 | 0.53 | 1.28 | 51.8 |
| Bavaria (Ester Mountains) | $\Delta\xi$ | 85 | -3.99 | 1.88 | 0.27 | 1.24 | 69.6 |
| Bavaria (Ester Mountains) | $\Delta\eta$ | 85 | -2.43 | 3.18 | 0.61 | 1.49 | 60.8 |
| Switzerland | $\Delta\xi$ | 35 | -7.66 | 7.53 | -0.12 | 2.69 | 35.8 |
| Switzerland | $\Delta\eta$ | 35 | -3.87 | 3.87 | 0.58 | 1.85 | 40.6 |